

MSEC2017-2721

INDUCTION HARDENING PROCESS WITH PREHEAT TO ELIMINATE CRACKING AND IMPROVE QUALITY OF A LARGE PART WITH VARIOUS WALL THICKNESS

Zhichao (Charlie) Li, and B. Lynn Ferguson

DANTE Solutions, Inc.
7261 Engle Road, Suite 105
Cleveland, Ohio, USA

Charlie.Li@Dante-Solutions.com

KEYWORDS

Induction hardening, spray quench, residual stress, phase transformation, quench crack, preheat.

ABSTRACT

During an induction hardening process, the electromagnetic field generated by the inductor creates eddy currents that heat a surface layer of the part, followed by spray quenching to convert the austenitized layer to martensite. The critical process parameters include the power and frequency of the inductor, the heating time, the quench delay time, the quench rate, and the quench time, etc. These parameters may significantly affect case depth, hardness, distortion, residual stresses, and cracking possibility. Compared to a traditional hardening process, induction hardening has the advantages of low energy consumption, better process consistency, clean environment, low distortion and formation of beneficial residual stresses. However, the temperature gradient in the part during induction hardening is steep due to the faster heating rate of the surface and the aggressive spray quench rate, which leads to a high phase transformation gradient and high magnitude of internal stresses. Quench cracks and high magnitude of residual stresses are more common in induction hardened parts than those of conventional quench hardening processes. In this study, a scanning induction hardening process of a large part made of AISI 4340 with varying wall thickness is modeled using DANTE. The modeling results have successfully shown the cause of cracking. Based on the modeling results, a preheat method is proposed prior to induction heating to reduce the in-process stresses and eliminate the cracking possibility. This process modification not only reduces the magnitude of the in-process tensile stress, but also converts the surface residual stresses from tension to compression at the critical inner corner of the part, which improves the service life of the part. The modified process has been successfully validated by modeling and implemented in the heat treating plant.

INTRODUCTION

During an induction hardening process, the part surface is heated using a medium or high frequency inductor. Once the desired depth of surface layer is austenitized, the part is spray quenched to convert the austenite layer to martensite. Compared to traditional furnace heating and liquid quenching processes, the induction hardening is more energy efficient because the heating time is short, and only the part surface is heated and austenitized. With the nonuniform temperature distribution in the part after heating, induction hardening also gives more options for part optimization such as improved case depth and beneficial residual stress distribution [1-3]. When austenite transforms to martensite, the material volume expands. During induction hardening, the core of the part doesn't transform to austenite, and the martensite transformation of the austenitized layer leads to compressive residual stresses in the surface. The compressive stresses have proven to be beneficial for both fatigue performance and wear resistance [4-6].

Stress evolution during steel heat treatment is a highly nonlinear process due to the phase transformations that occur. With phase transformations, the thermal and mechanical properties change, the material volume changes, the internal stresses within individual phases change, and the stresses between different phases also change. Simulation of heat treatment stresses and deformation is an emerging technology. Besides the variety and complexity of simulation algorithms, stress simulation requires large, accurate databases of thermal, metallurgical and mechanical properties of material phases over the entire range of temperatures experienced during processing.

Induction hardening is a transient thermal process. During induction hardening of steel components, the temperature gradient and phase transformations both contribute to the evolution of the internal stresses and part dimensional change. With induction hardening, the temperature difference between

the core and the surface has significant effect on the in-process stress and final residual stress. High core temperature (below austenitization temperature) will lead to higher surface compression in general due to the thermal contraction of the core once the surface martensitic transformation is complete. Several methods can be used to increase the core temperature before spray quenching, including slower heating rate, quench delay, and preheating. The preheat can be implemented by either lower power induction heating or furnace heating. The improvement and development of heat treatment simulation software make it much easier to understand the material response during the heat treatment process, most specifically concerning the generation of internal stresses and deformation. DANTE is a commercially available heat treatment software based on the finite element method that was developed to model carburization and conventional quench hardening processes for steel parts [7-8]. While DANTE was not designed to model the physics of induction heating processes, DANTE can be used to simulate the temperature field during induction heating by applying the internal heat flux (I^2R) based on the eddy current distribution in the part.

DESCRIPTION OF PART GEOMETRY, FEA MODEL, MATERIAL MODEL AND HARDENING PROCESS

Part Geometry and FEA Model

The part used in this study is simplified from a real industrial part, and the part dimensions are shown in Figure 1(a). The diameter of the part is 500 mm, the height is 250 mm. The bore is a square shape with its side length being 200 mm, so the wall thickness varies. The part inner corner fillet is 25 mm. The bore of the part is scanning induction hardened, and one quarter of the part is modeled to represent the entire part due to the symmetric geometries of the part and the inductor. The finite element mesh has 19,074 nodes and 16,850 hexagonal linear elements, as shown in Figure 1(b), with fine elements in the bore to catch the gradients of temperature, phase transformation and stresses during the entire process.

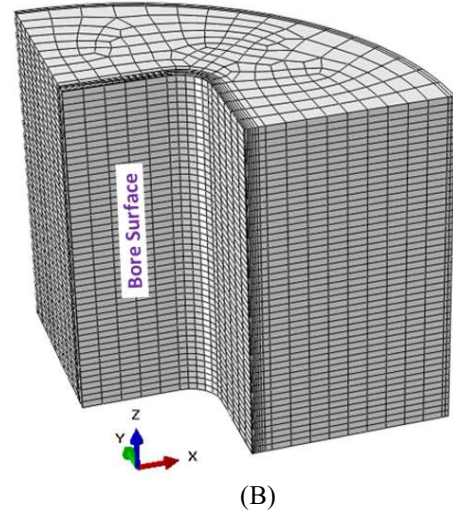
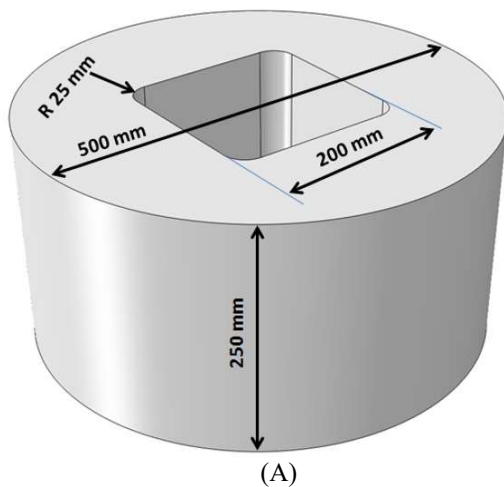


FIGURE 1 – (A) CAD MODEL OF THE PART, AND (B) FINITE ELEMENT MODEL.

A high percentage of cracking was observed in the corner fillet of the bore around its middle axial length region. The cracks initiate at the surface, and run along the axial direction. According to the cracking mode, the high tensile in-process in the circumferential direction should be the main cause of the cracking. As shown in Figure 1, more elements are used in the corner fillet to catch the in-process stress accurately.

Phase Transformation Kinetics

The cylinder used in this study is made of 4340 steel. Phase transformation models are required to model the heating and quench hardening processes [9]. The diffusive and martensitic transformation models in DANTE are described in equations (1) and (2) below.

$$\frac{d\Phi_d}{dt} = v_d(T)\Phi_d^{\alpha 1}(1-\Phi_d)^{\beta 1}\Phi_a \quad (1)$$

$$\frac{d\Phi_m}{dT} = v_m(1-\Phi_m)^{\alpha 2}(\Phi_m + \varphi\Phi_d)^{\beta 2}\Phi_a \quad (2)$$

where Φ_d and Φ_m are the volume fractions of individual diffusive phase and martensite transformed from austenite; Φ_a is the volume fraction of austenite; v_d and v_m are the mobilities of transformation; v_d is a function of temperature, and v_m is a constant; $\alpha 1$ and $\beta 1$ are the constants of diffusive transformation; and $\alpha 2$, $\beta 2$ and φ are constants of martensitic transformation. For each individual metallurgical phase, one set of transformation kinetics parameters is required.

Figure 2(a) is a continuous cooling dilatometry strain curve generated from the DANTE database representing austenite transformation to martensite for AISI 4340 steel. The horizontal axis in Figure 2(a) is temperature and the vertical axis is strain, so what is not shown is cooling time. The strain change due to martensitic transformation is clearly quantified.

When the dilatometry test sample cools to the martensitic formation starting temperature (M_s), its volume expands as the crystal structure changes from austenite's face centered cubic

(FCC) lattice to martensite's body centered tetragonal (BCT) lattice. Martensite's BCT structure has a lower density than austenite's FCC structure. The strain during transformation is a combination of thermal strain, phase transformation volume change, and strain induced by stresses generated during the transformation. The latter strain is referred to as Transformation Induced Plasticity (TRIP). The data obtained from this specific dilatometry test include coefficient of thermal expansion (CTE) for austenite and martensite, martensitic transformation starting and finishing temperature (M_s , M_f), transformation strain, and phase transformation kinetics (transformation rate) from austenite to martensite. These data are critical to the accuracy of modeling the internal stress and deformation caused by quenching.

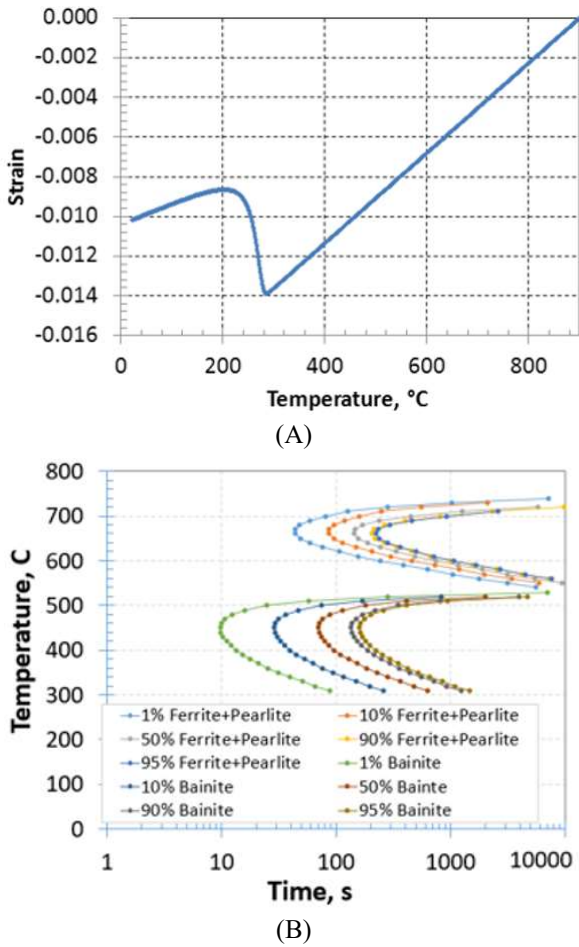


FIGURE 2 – PHASE TRANSFORMATION KINETICS. (A) DILATOMETRY DIAGRAM OF MARTENSITIC TRANSFORMATION, AND (B) TIME-TEMPERATURE-TRANSFORMATION (TTT) DIAGRAM.

Diffusive transformations are also characterized by dilatometry tests. A series of dilatometry tests with different cooling rates are required to fit a full set of diffusive and martensitic phase transformation kinetics parameters. Once the

full set of phase transformation kinetics parameters are fit from dilatometry tests, isothermal transformation (TTT) and continuous cooling transformation (CCT) diagrams can be generated for users to review. TTT/CCT diagrams are not directly used by DANTE phase transformation kinetics models, but they are useful because users can see the hardenability of the material graphically. Figure 2(b) is an isothermal transformation diagram (TTT) for 4340 steel created from the DANTE database.

Induction Hardening Process Description

Figure 3 shows schematically the scanning induction hardening process set-up using a simplified 2D model. The left side is the bore surface, and the right side is the outer surface of the part. The contour plot of the part is the temperature distribution, with red color representing higher temperature, and blue color representing lower temperature. The inductor is located inside the bore as shown. Neither the inductor nor the part rotates during the process because of the non-circular geometry feature of the bore. The width of the inductor is 50.8 mm in the axial direction, and its travel speed is 1.27 mm/s upward relative to the part in the axial direction as shown. Angled nozzles are designed on the bottom of the inductor to spray quench the heated bore. A water polymer solution is used as the quenching medium. The gap between the bottom of the inductor and the spray zone is 12.7 mm. With the travel speed being 1.27 mm/s, the quench delay is 10 seconds ($12.7 \text{ mm} / 1.27 \text{ mm/s}$). The quench delay time is an important process parameter in induction hardening process, because the temperature inside the part after heating is nonuniform, and thermal conduction during the delay can significantly change the temperature profile before the part is quenched.

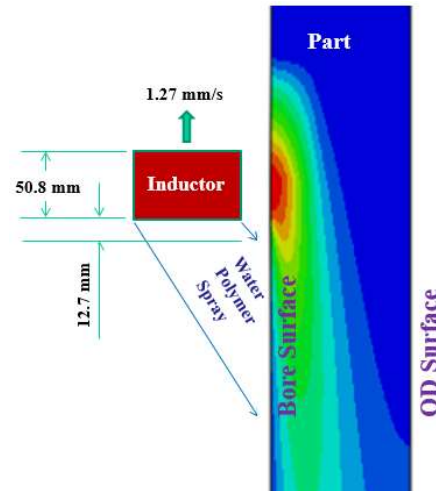


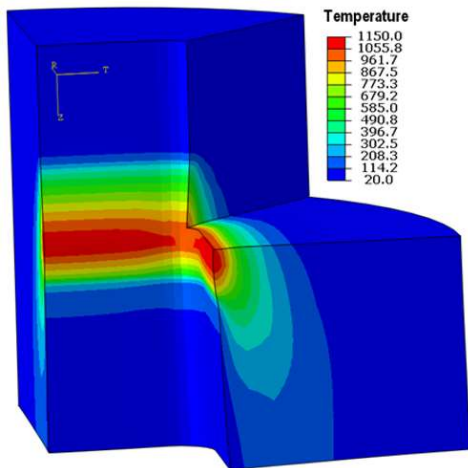
FIGURE 3 – SCHEMATIC SETTING OF THE INDUCTION HARDENING PROCESS.

At the beginning of the process, the top of the inductor aligns with the bottom of the part. The power of the inductor is turned off once it exits the part, so the entire scanning heating process takes 236.85 seconds. Once the power is turned off, an

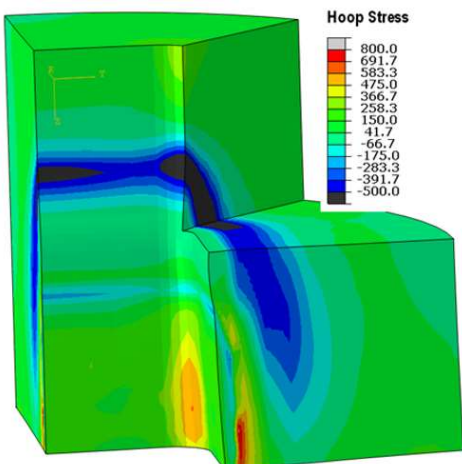
extra 60 seconds is applied to complete the transformation of austenite to martensite, then the part is removed to cool in air. The minimum required case depth is 6.5 mm.

MODELING RESULT ANALYSIS

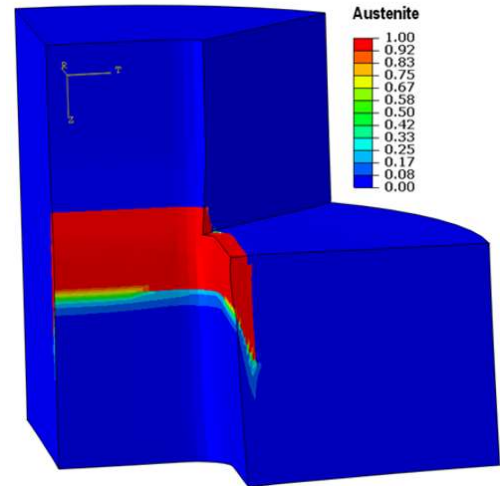
Snapshots of temperature, stress and phase distributions at 136.6 second of the hardening process are shown in Figure 4. A portion of the model is removed so the predicted results under the surface of the corner fillet can be viewed. The predicted displacements are magnified by 10 times in the contour plots for easier viewing. The surface temperature of the part is about 1150° C after scanning induction heating, and the temperature at the corner fillet is lower due to its geometric feature, as shown in Figure 4(a). The circumferential (hoop) stress contour in Figure 4(b) is plotted using a local cylindrical coordinate system, so the circumferential stress at the corner fillet is in the tangential direction. Figure 4(c) shows the austenite phase that is produced by the heating at this time, and Figure 4(d) shows the martensite that has formed as a result of the spray quenching. The stress state in Figure 4(b) is a combined effect due to both the thermal gradient and phase transformations.



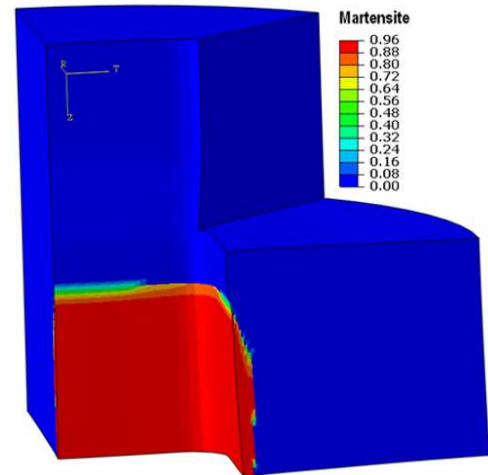
(A)



(B)



(C)

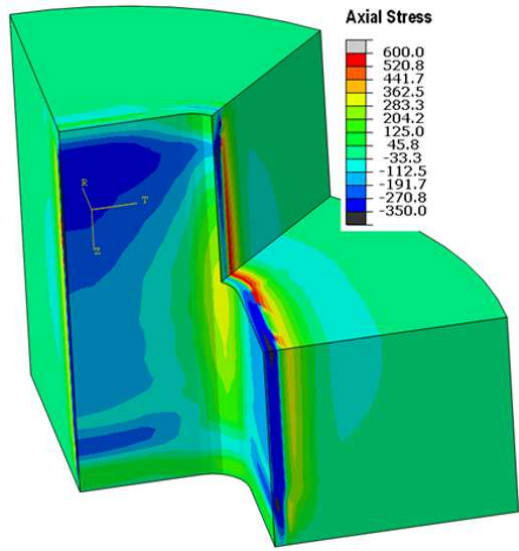


(D)

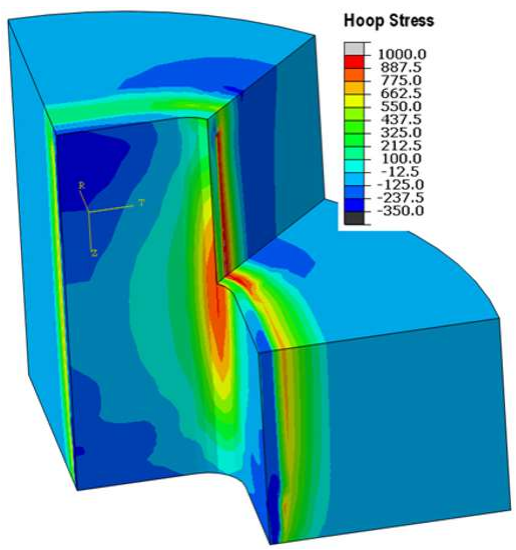
FIGURE 4 – (A) TEMPERATURE, (B) CIRCUMFERENTIAL STRESS, (C) AUSTENITE, AND (D) MARTENSITE DISTRIBUTIONS AT 136.6 SECOND DURING INDUCTION HARDENING PROCESS.

The predicted axial and circumferential stresses, martensite and radial displacement at the end of the hardening process (as-quenched condition with the part cooling to room temperature) are shown in Figure 5. The case depths are 8 mm and 10 mm, respectively at the corner fillet and flat bore surfaces, as shown in Figure 5(c). The predicted residual stresses in the axial direction, Figure 5(a), at the flat bore surface are compressive and range from about -100 MPa to -350 MPa. These values compare to residual tension of ~250 MPa at mid-height of the corner fillet surface. In Figure 5(b), the predicted circumferential stress at mid-height of the corner fillet surface is ~1000 MPa in tension, which suggests a high potential for cracking. High residual tension at the fillet surface also increases the cracking possibility during service as the fatigue performance is reduced. Under the hardened case, residual tension is predicted in both the

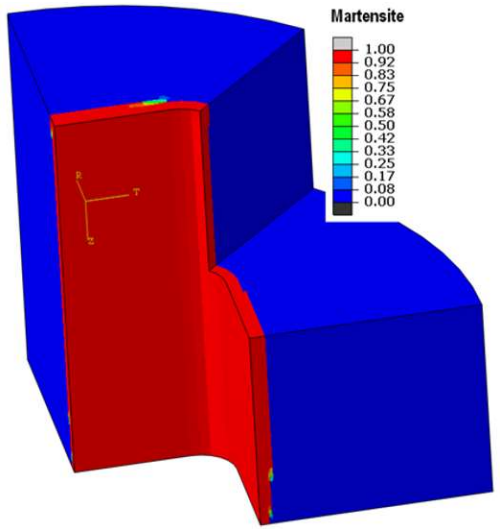
hoop and axial directions. However, the cracking potential under the case is low relative compared to the surface location because of greater energy required to initiate a sub-surface crack. Radial displacement is shown in Figure 5(d) using the cylindrical coordinate system. Radial shrinkage is predicted, with around 80 μm to 100 μm for the OD surface, and 200 μm for the bore. Over 300 μm radial shrinkage is predicted at the middle height of the corner fillet. Because this is a scanning process, residual stress, phase and displacement are different between the top and bottom of the part.



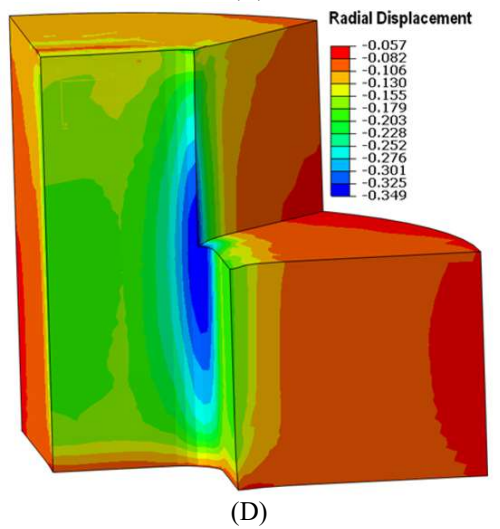
(A)



(B)



(C)



(D)

FIGURE 5 – (A) AXIAL STRESS, (B) CIRCUMFERENTIAL STRESS, (C) MARTENSITE, AND (D) RADIAL DISPLACEMENT DISTRIBUTIONS AT THE END OF INDUCTION HARDENING PROCESS.

During the induction hardening process, both the thermal gradient and phase transformations contribute to the stress state. Four points shown in Figure 6 are selected to understand the stress evolution process. The four points, A, B, C, and D, are located at mid-height of corner fillet, with depths of 0.0, 3.5, 10.0 and 37.0 mm, respectively from the surface. Points A and B are in the hardened case, point C is under the case, and point D is in the core.

Figure 7 shows the sequence of events that occurs as the fillet is heated, austenite forms and then transforms to martensite. During heating, the bore surface experiences compression due to the surface thermal expansion and constraint by the cold body, Figure 7(c). When austenite forms at the bore surface, compression drops because of the phase change, and the low strength of austenite and the resulting transformation induced

plasticity (TRIP). The gap between the inductor and the spray leads to quench delay, and the surface temperature at point A drops from 1050 to 800 °C due to the 10 second quench delay before being spray quenched, see Figure 7(a). The main reason for the temperature drop is thermal conduction from hot section into the cold body. The gap between the inductor and the spray, or dwell time, can have significant effect on the quenching results. After martensitic transformation is completed along line A-D, the hoop stresses at the surface point A and inner point C increase significantly by stress concentration due to temperature balance. An axial surface crack is expected to form near mid-height of the corner fillet, and similar cracks have been observed during bore hardening of parts with non-uniform wall thicknesses.

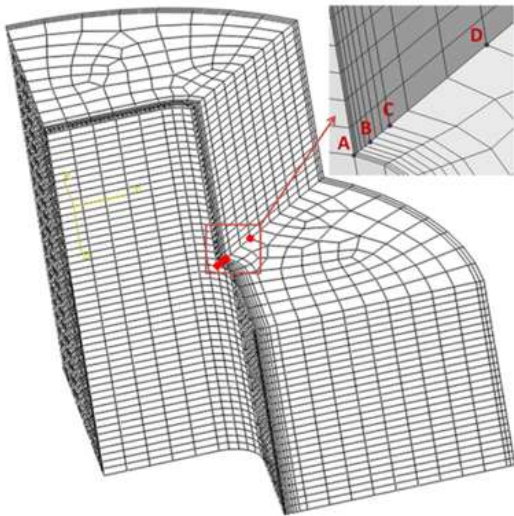


FIGURE 6 – POINTS SELECTED FOR POST-PROCESSING THE HISTORIES OF THE MATERIAL REPOSE DURING INDUCTION HARDENING.

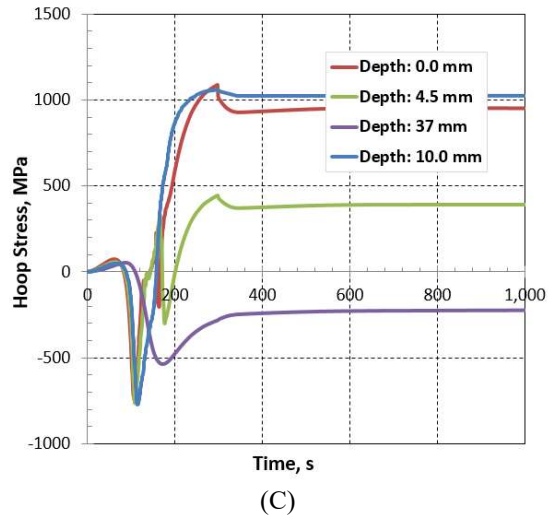
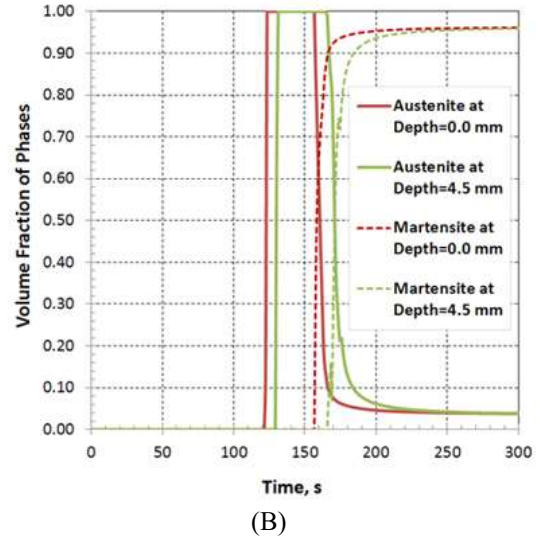
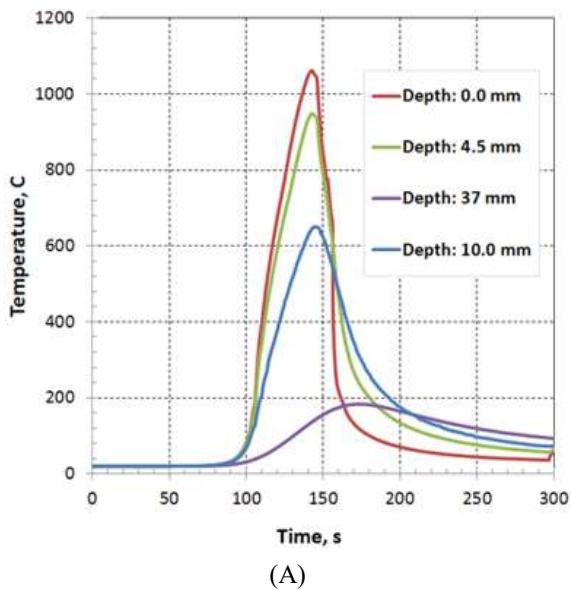


FIGURE 7 – EVOLUTIONS OF (A) TEMPERATURE, (B) VOLUME FRACTIONS OF PHASES, AND (C) CIRCUMFERENTIAL STRESS DURING INDUCTION HARDENING PROCESS.

PROCESS IMPROVEMENT BY MODELING

The modeling results described in the previous section clearly showed the significant effect of the thermal gradient and phase transformation on the in-process stress evolution and residual stress magnitude. Figure 7(c) shows that temperature balancing after the martensitic transformation is completed (between 200s and 300s during the process) leads to high concentrated heating stress in the corner fillet. During the entire induction heating and cooling process, the OD surface of the part remains cold. If the OD surface or the part body is heated to a temperature without affecting its metallurgical phase prior to induction heating, the thermal shrinkage of the body once martensitic transformation is complete can squeeze the bore and change its stress state. The preheat process prior to induction

hardening can be implemented by either furnace heating or induction heating with low power [10, 11]. In this study, the part is preheated to 200° C in a furnace, and the power applied to the inductor during hardening process is reduced to maintain the same case depth, while the frequency of the inductor remains the same. The process is modeled using DANTE, and the predicted residual stresses at the end of the hardening process are shown in Figure 8. The tensile residual stress predicted at the critical location is about 200 MPa in the circumferential direction, comparing to about 1000 MPa from the original process. The preheat process makes it possible to control the in-process and residual stresses at critical locations of the part.

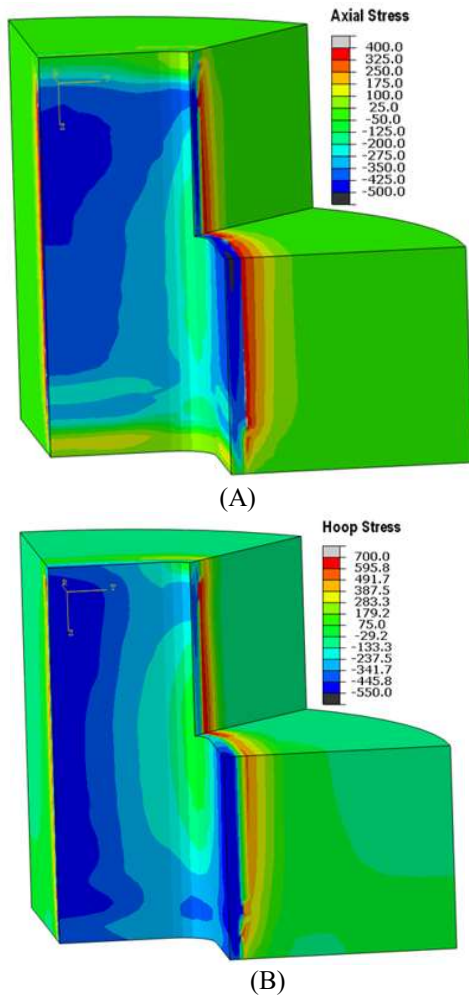


FIGURE 8 – (A) AXIAL RESIDUAL STRESS, AND (B) CIRCUMFERENTIAL RESIDUAL STRESS DISTRIBUTION PRODUCED BY INDUCTION HARDENING WITH PREHEATING.

To further understand the effect of preheating on the in-process and the residual stresses in the part, the history plots of temperature, phase transformation and stress are plotted in Figure 9 for the induction hardening process with preheating.

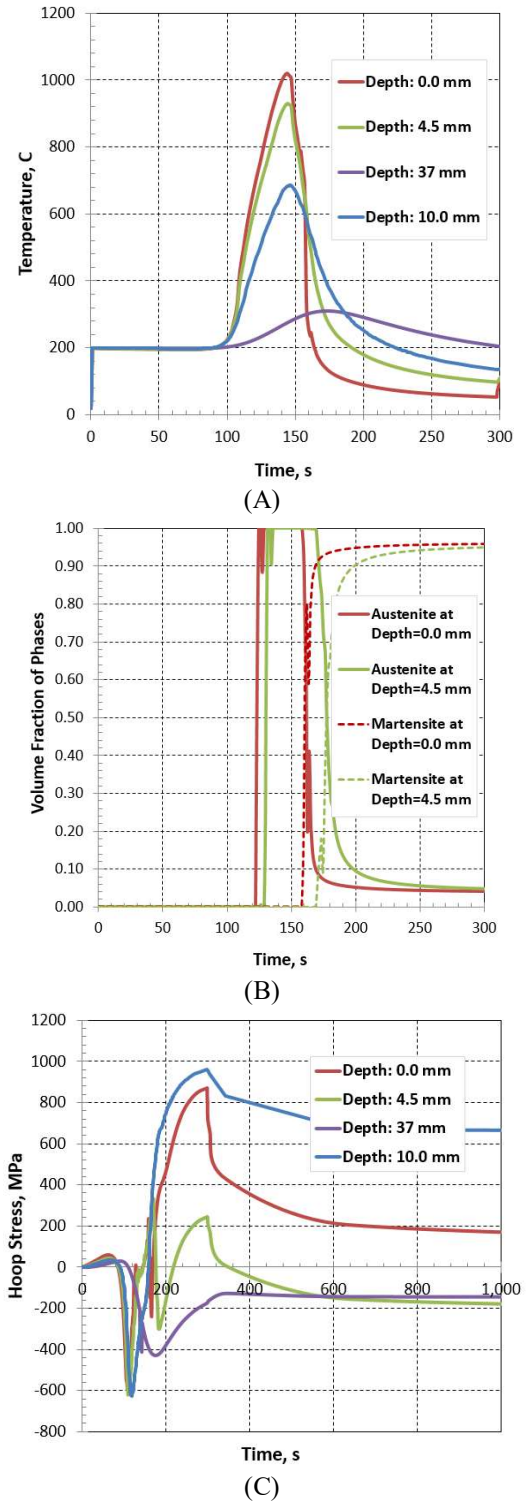


FIGURE 9 – EVOLUTIONS OF (A) TEMPERATURE, (B) VOLUME FRACTIONS OF PHASES, AND (C) CIRCUMFERENTIAL STRESS DURING INDUCTION HARDENING PROCESS WITH PREHEAT.

The predicted peak stress at the surface is 850 MPa, compared to 1080 MPa from the original process, as shown in Figure 7 and Figure 9, which makes significant difference on the possibility of cracking. The process has been implemented successfully to harden parts without observing cracked parts.

SUMMARY

The scanning induction hardening process of a large part with varying wall thickness was modeled using the finite element based software DANTE. The modeling results provided intuitive understanding of the nonlinear behavior of temperature, phase transformation and stress evolutions during the process. Preheating the part prior to induction hardening changes the temperature distribution, which affects both the in-process and residual stress distribution in the part by thermal shrinkage. The effect of preheat is both part geometry and process dependent, so the preheat process needs to be implemented carefully to realize the beneficial effect without damaging mechanical and metallurgical properties of the part.

REFERENCES

- [1] Induction Heating and Heat Treating, Vol 4C, ASM Handbook, V. Rudnev and G. Totten, eds., ASM Intl., 2014.
- [2] Goldstein, R., Nemkov, V., Madeira, R.: Optimizing Axle-Scan Hardening Inductors. *Industrial Heating*, 12, 2007.
- [3] Golovin, G., Residual Stresses and Deformation during High-Frequency Surface Hardening, Mashghiz, Moscow, 1962 (in Russian).
- [4] Jahanian. S., Thermoelastoplastic and Residual Stress Analysis during Induction Hardening of Steel, *Journal of Materials Eng. and Performance*, V. 4, Issue 6, 1995.
- [5] Li, Z., Ferguson, B., Goldstein, G., Nemkov, V., Jackowski, J., and Fett, G.: Modeling Stress and Distortion of Full-float Truck Axle during Induction Hardening Process, 27th ASM-HTS Conference, 2013.
- [6] Grum, J., Overview of residual stresses after induction surface hardening. *International Journal of Materials and Product Technology*, Volume 29, no.1-4, 2007.
- [7] Ferguson, B., Freborg, A., and Petrus, G., “Software Simulates Quenching”, *Advanced Materials and Processes*, H31-H36, August (2000).
- [8] Dowling, W., et al., “Development of a Carburizing and Quenching Simulation Tool: Program Overview,” 2nd Int. Conference on Quenching and Control of Distortion, eds, G. Totten, et al., ASM Int., 1996.
- [9] Li, Z., Ferguson, B., and Freborg, A., “Data Needs for Modeling Heat Treatment of Steel Parts”, *Proceedings of Materials Science & Technology Conference*, 2004, pp. 219-226
- [10] Li, Z., Freborg, A., and Ferguson, B., “Effect of Preheat on Improving Beneficial Surface Residual Stresses during Induction Hardening Process”, *Proceedings of the ASME 2016 International Manufacturing Science and Engineering Conference*, June 27 – July 1, 2016, Blacksburg, Virginia, USA.

- [11] Li, Z., “Innovative Induction Hardening Process with Preheating for Improved Fatigue Performance of Gear Component”, AGMA Fall Technical Meeting, September 15 – 17, 2013, Indianapolis, USA.